Construction and Building Materials 127 (2016) 369–382

Contents lists available at ScienceDirect

Construction and Building Materials

journal homepage: www.elsevier.com/locate/conbuildmat

Effect of fibres addition on the physical and mechanical properties of asphalt mixtures with crack-healing purposes by microwave radiation

J. Norambuena-Contreras [a,*], R. Serpell [b], G. Valdés Vidal [c], A. González [d], E. Schlangen [e]

[a] LabMat-UBB, Department of Civil and Environmental Engineering, University of Bío-Bío, Concepción, Chile
[b] Department of Construction Engineering and Management, School of Engineering, Pontificia Universidad Católica de Chile, Santiago, Chile
[c] Department of Civil Engineering, University of La Frontera, Temuco, Chile
[d] Faculty of Engineering, Universidad del Desarrollo, Avenida Plaza 680, Las Condes, Santiago 7610471, Chile
[e] Microlab, Faculty of Civil Engineering and Geosciences, Delft University of Technology, Delft 2628 CN, The Netherlands

HIGHLIGHTS

- Fibres distribution and mechanical behaviour of asphalt mixtures were analysed.
- Effect of environmental conditions on particle loss of mixtures was evaluated.
- Fibres presented a good spatial distribution into the asphalt mixture samples.
- Asphalt mixtures with higher fibre content may produce dense clusters.
- Fibres did not contribute to improve the mechanical properties of the mixtures.

ARTICLE INFO

Article history:
Received 6 June 2016
Received in revised form 7 September 2016
Accepted 4 October 2016
Available online 8 October 2016

Keywords:
Asphalt mixture
Physical properties
Mechanical properties
Fibres distribution
X-ray microtomography

ABSTRACT

Microwave heating is regarded as a promising technique to promote crack-healing of asphalt mixtures reinforced with steel wool fibres. In addition to serving as a heat source when subject to microwave radiation, steel wool fibres are expected to affect the physical and mechanical properties of the asphalt pavements. However, it is not clear what this effect is, and what is the optimum fibre content that can provide effective crack-healing without having a negative impact on other relevant mixture properties. This paper reports a study of the steel wool fibres spatial distribution and their influence on the physical and mechanical properties of asphalt mixtures. For this purpose, five different dense asphalt mixtures, with the same aggregates gradation and bitumen content, but with five different percentages of steel wool fibres were manufactured. Then, their mechanical properties such as particle loss resistance in dry and wet conditions, and stiffness modulus and cracking resistance in Mode I of fracture at four different temperatures were evaluated. Samples of these mixtures were examined using Scanning Electron Microscopy and analysed using X-ray micro computed tomography to study the condition and distribution of fibres within the bitumen matrix. Microscopy results showed that fibres can be damaged during the mixing and compaction processes. A larger variability in the local distribution of fibres for mixtures incorporating a higher fibre content was observed in the tomography analysis, with presence of fibre clusters more than double of the average fibre content of the mixture. Although addition of fibres appears to reduce the bulk density of mixtures, according to tomography analysis differences in average porosity between samples were not statistically significant. Finally, it was confirmed that regardless of test temperature, steel wool fibres did not have a relevant influence on the improvement of particle loss resistance, stiffness modulus and cracking resistance of asphalt mixtures.

1. Introduction

An asphalt mixture is a material composed of aggregates and bitumen, and it is one of the most commonly used materials in pavement construction worldwide. As a reference,

* Corresponding author.
E-mail address: jnorambuena@ubiobio.cl (J. Norambuena-Contreras).

http://dx.doi.org/10.1016/j.conbuildmat.2016.10.005
0950-0618/

within the 18,000 km of paved roads in Chile, there are currently 16,000 km paved with asphalt mixtures [1]. However, environmental conditions combined with traffic loads contribute to premature deterioration of asphalt pavement materials, reducing their mechanical strength and durability over time. The main environmental factors affecting durability of asphalt mixtures are ageing [2], water damage [3] and thermal cracking [4]. These factors may have a negative influence on the stiffness of bitumen and on the particle loss resistance of asphalt mixtures. With the aim of improving the mechanical properties of asphalt mixtures against environmental damage, different types of fibres can be incorporated to the matrix of mixtures [5]. Many types of fibres are available for incorporation into asphalt mixtures [6]. For example, cellulose and mineral fibres [7]; polypropylene and polyester fibres [8]; and various polymers, steel wool, and other waste fibres [9] are sometimes added to asphalt mixtures. Metallic fibres in asphalt mixtures are known for enhancing their strength and fatigue characteristics while increasing their ductility [10]. In addition, they may contribute to prevent the formation and propagation of cracks [11], and, since the fibre material has high tensile strength relative to asphalt mixtures, they may improve the cohesive and tensile strength of mixtures [5]. Hence, fibre-reinforced asphalt mixtures may have a good resistance to ageing, moisture damage and resistance to cracking [6]. Metallic fibres (steel wool) can also be used to modify the electrical [12] and thermal conductivities [13] of mortar and asphalt mixtures, and to heal the open cracks via electromagnetic induction heating [12–19]. It is well known that asphalt pavements present self-healing properties when they register high temperatures during summer season, which means that cracks in the road can be closed by themselves. This happens because the viscosity of bitumen is temperature dependent. Thus, when bitumen reaches a temperature threshold (30–70 °C), which is different for each type of bitumen, it starts flowing through micro-cracks opened in the pavement, in a sort of capillary flow [16]. Consequently, metallic fibres can be used to increase heating rates of asphalt mixtures considering that these fibres can absorb and conduct more thermal energy than the other components of the mixture, aggregates and bitumen. Crack-healing of asphalt mixtures using electromagnetic heating consists on adding metallic fibres (steel wool) to the mixture, which are electrically conductive and magnetically susceptible to an electric field [17]. Therefore, with the help of an electromagnetic radiation device such as a microwave oven, it is possible to heat the asphalt mixtures with fibres, melting the bitumen and repairing opened cracks existing in the pavement. Microwave radiation is a heating technique where asphalt materials are exposed to alternating electromagnetic fields, in the order of Megahertz [20]. In previous researches, this microwave heating technique has shown potential for the crack-healing of asphalt mixtures [21] and polymeric composite materials [22] reinforced with steel wool fibres, although it has not been deeply explored.

This paper has been prepared in the frame of a research project focused on the development of a new fibre-reinforced asphalt mixture with self-healing properties via microwave heating [23]. For this reason, electrically conductive steel wool fibres have been mixed into the asphalt mixture. The addition of fibres may influence the physical and mechanical behaviour of the material. However, the mechanisms involved on these effects and the relationship between them and the fibre content needed for self-healing purposes requires further study. For these reasons, the steel wool fibres spatial distribution and their influence on the physical and mechanical properties of asphalt mixtures have been studied. To reach these objectives, five different dense asphalt mixtures, with the same aggregates gradation and bitumen content, but with five different percentages of steel wool fibres have been evaluated in the laboratory.

2. Materials and methods

2.1. Materials

A dense asphalt mixture has been used in this research. The mixture composition is shown in Table 1. The aggregates consisted of coarse aggregate or gravel (size between 5 and 12.5 mm, and density 2.779 g/cm^3), fine aggregate or sand (size between 0.08 and 5 mm and density 2.721 g/cm^3), and filler (size < 0.08 mm and density 2.813 g/cm^3). The bitumen used was type CA24 with a penetration of 5.6 mm at 25 °C and density 1.039 g/cm^3, according to Chilean Standard [24]. Properties of the bitumen used are shown in Table 2. In addition, steel wool fibres (see Fig. 1(a)) were added to the asphalt mixture. The material of the fibres was a low carbon steel with density 7.180 g/cm^3. The fibres had an average diameter of 0.157 mm with average aspect ratio of 30 and initial length ranged from 2 to 8 mm (see fibres length distribution in Fig. 1(b)), which means that both short and long fibres were added to the asphalt mixture matrix. Finally, different percentages of fibres were added to the mixture: 0%, 2%, 4%, 6% and 8%, by total volume of bitumen, to obtain five different types of asphalt mixtures: one asphalt mixture without fibres (reference mixture)

Table 1
Composition of the asphalt mixture.

Sieve size (mm)	Aggregate mass % retained	Cumulative aggregate mass % retained
12.5	16	16
10	13	29
5	24	53
2.5	16	69
0.63	17	86
0.315	4	90
0.16	3	93
0.08	2	95
<0.08	5	100
Bitumen CA24	(% of mass in the mixture)	5.3
Steel wool fibres (% volume of bitumen)	Length range (mm)	Average diameter (mm)
2% fibres 4% fibres 6% fibres 8% fibres	2–8	0.157

Table 2
Properties of the bitumen CA-24.

Experimental tests	Result	Standard Specifications
Absolute Viscosity at 60 °C, 300 mm Hg (P)	3077	Min 2400
Penetration at 25 °C, 100 g. 5 s. (0.1 mm)	56	Min 40
Ductility at 25 °C (cm)	>150	Min 100
Spot test hep./xil. (%xylene)	<25	Max 30
Cleveland Open Cup Flash Point (°C)	332	Min 232
Softening Point R&B (°C)	51	To be reported Min 99
Trichloroethylene solubility (%)	99.9	–
Penetration Index	−0.7	−1.5 a + 1.0
RTFOT		
Mass Loss (%).	0.00	Max 0.8
Absolute Viscosity at 60 °C, 300 mmHg (P)	7475	To be reported Min 100
Ductility at 25 °C, 5 cm/min (cm)	150	–
Durability Index	2.4	Max 3.5

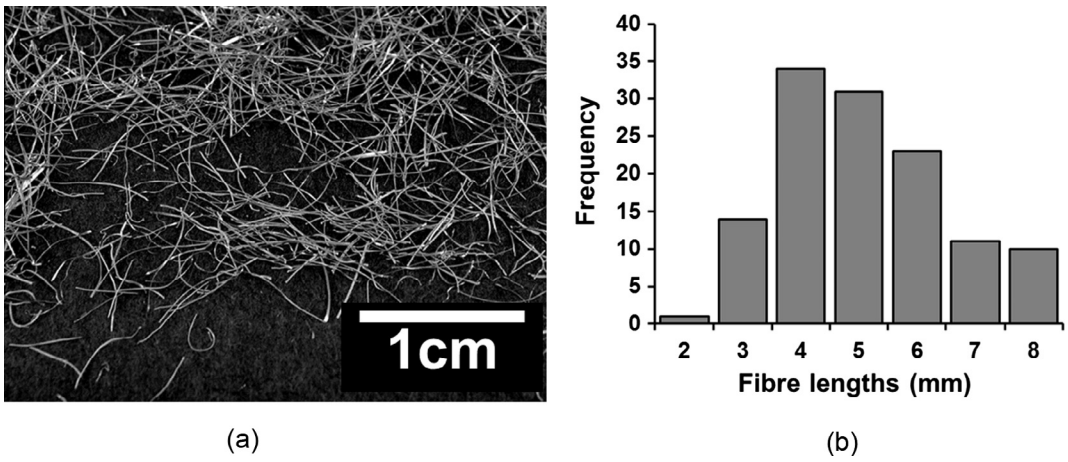

Fig. 1. (a) Steel wool fibres used and (b) length distribution of steel wool fibres.

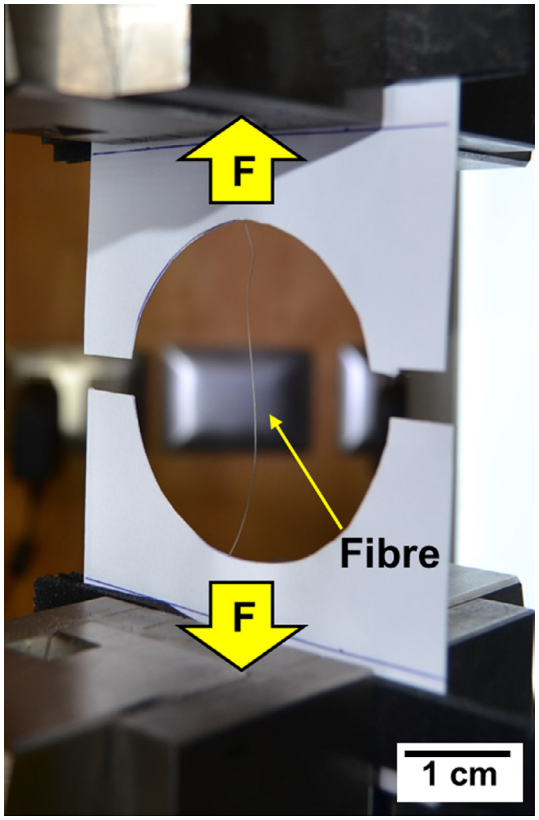

Fig. 2. Tensile strength set-up for individual steel wool fibre.

and four asphalt mixtures reinforced with different fibres contents, but using the same aggregates gradation and bitumen content.

2.2. Test specimens preparation

The materials were mixed in a laboratory planetary mixer at a mixing speed of 100 rpm. The amount of material in each mixture was approximately 6 kg. Materials were first heated at 150 °C during approximately 2 h and then mixed for approximately 3.5 min. The raw materials were added into the bowl in the following order: first, bitumen and steel wool fibres; second, coarse aggregate; third, fine aggregate and finally, filler. The asphalt batch was used to manufacture cylindrical Marshall specimens of approximately 100 mm diameter and 60 mm height. These test specimens were compacted using a Marshall compactor, giving 75 blows to each face of the test specimens. Finally, a selection of cylindrical Marshall specimens were cut through their diameter using a cutting saw for asphalt, to make Fenix test samples (half Marshall Sample). A notch with thickness and depth of about 5 mm was cut in the Fenix test samples; the notch was cut at the midpoint from the central axis of the sample (Fig. 4). In total, approximately 250 Marshall specimens were manufactured for this study.

2.3. Morphological characterization of steel wool fibres

The average length of 120 individual steel wool fibres was measured by taking photographs under an optical microscope at 8× magnification, and by measuring the individual fibres length with an image processing program (ImageJ®). The average diameter of the fibres was calculated from 10 individual fibres using a calibrated digital micrometre (Table 1). In addition, the morphology of individual fibres was studied using a Scanning Electron Microscope (JEOL JSM-6610/LV). Finally, the fibres were also examined after the mixing and compaction processes by dissolving the bitumen in toluene and extracting them with a magnet.

2.4. Tensile strength of the individual fibres

The tensile strength of individual steel wool fibres was measured via a static universal testing machine Zwick/Roell with 20 kN load cell. After measuring their diameter each individual fibre was glued by its ends onto a paper form of 80 × 100 mm resulting in a test length of approximately 55 mm and then tested until failure (see Fig. 2). All the tests were done at a speed ratio of 0.5 mm/min. The maximum force resisted by the fibres was defined as the average value obtained from 10 fibres samples.

2.5. Bulk density and air voids content

With the aim of evaluating physical properties of asphalt mixtures with and without addition of fibres, bulk density and air voids content of all Marshall specimens were determined. Bulk density of each specimen was calculated as the relationship between the dry mass and the real volume including air voids determined by water-submerged weight. Air voids content of each specimen was calculated based on the previous calculation of bulk density. Hence, as the exact percentage of materials and their density for each asphalt mixture type were known, the

theoretical maximum density without voids for each specimen was found. The air voids content (AVC) of each test sample was calculated as:

$$AVC(\%) = \frac{\rho_{max} - \rho_b}{\rho_{max}} \quad (1)$$

where ρ_b is the bulk density of each specimen in g/cm^3, and ρ_{max} is the theoretical maximum density without voids of each specimen in g/cm^3. The bulk density and air voids content were calculated from the average of 30 test samples for each percentage of fibres.

2.6. X-ray computed tomography (CT scan)

In order to analyse the spatial distribution of the steel wool fibres inside the asphalt mixture specimens, X-ray micro computed tomography was employed. With this purpose, cylindrical specimens of approximately 25 mm in diameter and 12 mm in height were cut from sections of Marshall specimens. The X-ray microtomography scans were obtained using a Bruker SkyScan 1272 scanner. The scanner was operated at 100 kV and 100 μA and images were reconstructed at a spatial resolution of 26.8 μm (voxel side). Classification of voxels as phases present in the mixture (i.e.

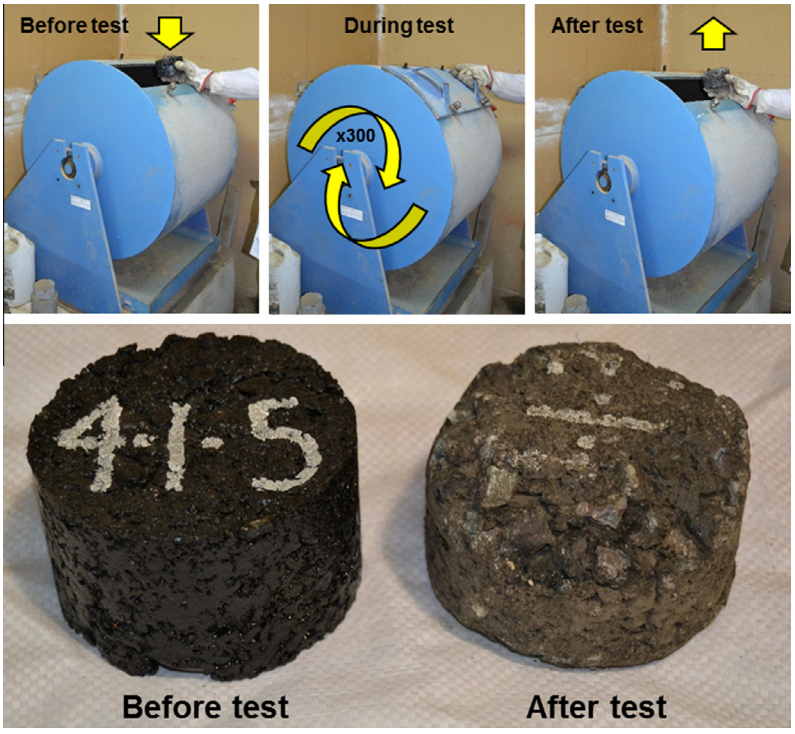

Fig. 3. Particle loss set-up and example of particle loss in a dry specimen with 4% fibres.

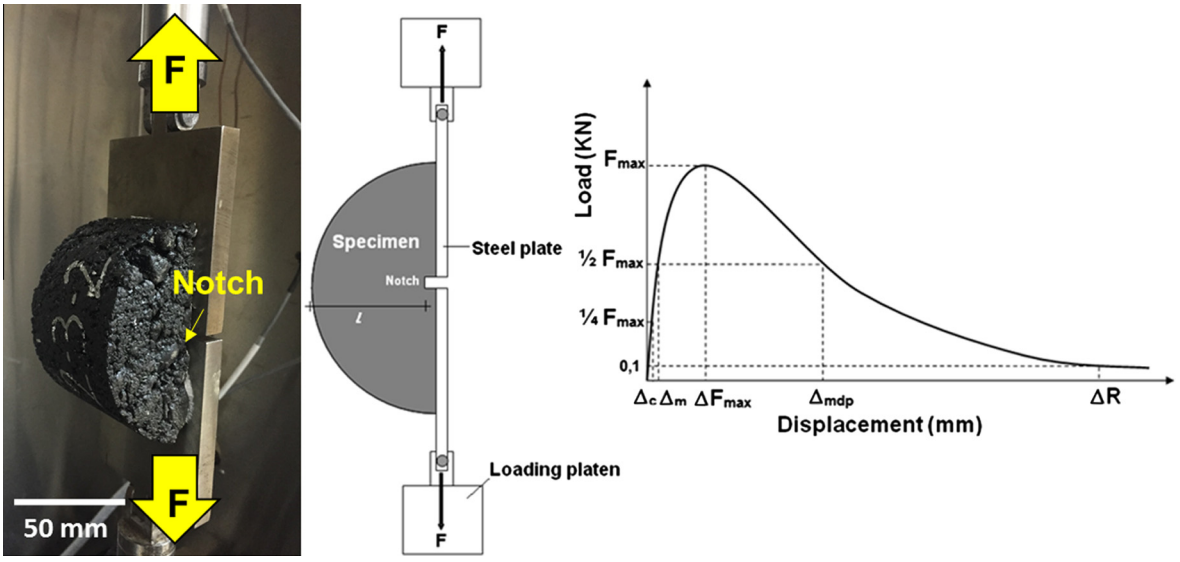

Fig. 4. Fenix test set-up and load-displacement output curve.

voids, bitumen, aggregate and fibres) was achieved by segmenting based on voxel intensity values, which are proportional to average density of the specimen within the volume mapped by each voxel. Transition between air and solids was readily apparent as a deep in the histogram of the voxel values (a null in the derivative of the histogram values). Transition from bitumen to aggregate was less apparent, and was identified as the first maximum in the derivative of the histogram at voxel values above the air-solids transition. Using this criteria, the estimated bitumen volume fraction of the solids was close to the expected bitumen content of the mixtures for most of the samples. Due to the relatively low spatial resolution of the reconstruction, as compared to the width of the fibres, it was not possible to identify a definitive marker for the transition between aggregate and fibres, since voxels close to the surface of the fibres have intensity values ranging continuously between that of the bitumen and that of the steel fibres. Although this implies that the exact fibre content in each specimen cannot be determined from the reconstruction data alone, it does not affect the analysis of the distribution of fibres within the specimens, that is, the variation of the local content of fibres throughout the specimen. Consequently, the transition between aggregate and fibres was fixed at an intensity value that resulted on an average fibre volume fraction in the bitumen most closely approaching the design mixture fraction (i.e. 0.02, 0.04, 0.06 and 0.08). The segmentation intensities resulting from the described criteria were similar across specimens. With this simple method, aggregates, fibres, bitumen and air voids could be readily separated. The classification and statistic of phases was performed using ad-hoc Python scripts, using modules NumPy and SciPy. Moreover, for the determination of phase fractions, only the inner 55% of the scanned volume of each specimen was included in the analysis, in order to avoid effects related to damage of surfaces during specimen shaping and handling, which often results in fragments detaching from the specimen. With the aim of obtaining a measure of sample variance, the analysed volumes were sub-sampled in halves along different geometries to obtain 6 data points per specimen. Phase fractions reported for each mixture design are thus the average results from 12 sub-samples from 2 specimens, with sub-samples having the same volume across specimens and mixtures. Distribution of fibre content within asphalt mixtures was analysed by sub-sampling the full scanned volume of each specimen in pieces encompassing a fixed volume of bitumen. This was achieved by implementing an auto-adjustable sub-sample volume in the analysis script. The target bitumen volume used was 0.125 cm^3 which corresponds to an average sub-sample volume of 1 cm^3 according to the mixture design. More than a 100 overlapping sub-samples were obtained from each scanned specimen volume using a 3D positioning grid with a spacing of 2.7 mm in each direction. Volumetric fibre fraction of bitumen was measured and recorded at each point to construct a distribution of fibre content.

2.7. Particle loss resistance

As one of the purposes of fibres in dense asphalt mixture would be to prevent the loss of aggregates in roads, the particle loss resistance test was chosen for characterizing the effect of fibres under two different environmental conditions. Particle loss resistance has been determined according to European Standard EN 12697-17: 2004 [25]. Marshall Test specimens were preconditioned under dry and wet conditions according to recommendation of Garcia et al. [26]. For the dry condition, specimens were placed in a temperature-controlled room at 20 °C for 24 h. For the wet condition, specimens were vacuum-saturated and then submerged in a 40 °C water bath during 120 h before testing. After the preconditioned period, each specimen was subjected to 300 revolutions at 30 rpm into the Los Angeles Machine without steel balls (see Fig. 3). The mass of the specimen before and after the test was registered and the Particle Loss (PL) was calculated using Eq. (2):

$$PL(\%) = \frac{w_i - w_f}{w_i} \tag{2}$$

where w_i is the initial specimen mass before the test, measured in kg and w_f is the final specimen mass after the test, measured in kg. For each type of fibre-reinforced asphalt mixture and condition 20 Marshall specimens were tested. In total, more than 160 Marshall specimens were tested.

2.8. Indirect tensile stiffness modulus measurements

The stiffness of the asphalt mixtures specimens was measured by means of the indirect tensile stiffness modulus test. Stiffness modulus has been determined according to European Standard UNE-EN 12697-26:2006 Annex C [27]. This methodology consists on doing an indirect tensile test on cylindrical Marshall specimens, applying sinusoidal loading pulses and resting periods to reach an established horizontal strain. Ten loading pulses were vertically applied on two orthogonal diameters. Stiffness modulus was obtained applying the Eq. (3):

$$SM = \frac{F \cdot (\upsilon + 0.27)}{(z \cdot h)} \tag{3}$$

where SM is the measured Stiffness Modulus in MPa, F is the maximum vertical load applied in N, z is the horizontal strain amplitude in mm, h is the average thickness of the specimen in mm, and v is the Poisson's ratio (0.36 according to [28]). Finally, in order to evaluate the influence of fibre content and test temperature on the stiffness modulus of asphalt mixtures, three specimens for each asphalt mixture type (see Table 1) were tested at four different temperatures: 0, 10, 20 and 40 °C. In total, more than 60 Marshall specimens were tested.

2.9. Cracking resistance using Fenix Test

Cracking resistance of asphalt mixtures was analysed by using Fenix Test. The Fenix Test is a non-traditional procedure developed at the Roads Laboratory of the Technical University of Catalonia. This mechanical test simulates the Mode I of fracture, which is the main cracking mechanism of asphalt pavements [29]. This procedure consists on applying a direct tensile load on half-Marshall specimen until the propagation of a previously induced crack starts. Before the test, Fenix samples were fixed to two steel plates and then conditioned at established temperatures. Plates were fixed to the test machine pistons by ball and socket joints, and then they were vertically moved at a constant rate of 1 mm/min. Force and piston displacement values were recorded simultaneously until the load reached 0.1 kN, when the test was considered as finished. Several mechanical parameters that characterize cracking resistance of asphalt mixtures were obtained from the load-displacement curve (see Fig. 4). Mechanical parameters obtained from the Fenix Test are the following:

- *Maximum tensile force (Fmax):* Maximum force in kN resisted by the Fenix sample when subjected to tensile loading
- *Tensile stiffness index (TSI):* This parameter defines an indicator of the stiffness level of asphalt mixture.

$$TSI = \frac{1/2Fmax - 1/4Fmax}{\Delta m - \Delta c} \tag{4}$$

where TSI is the Tensile Stiffness Index in kN/mm, F_{max} is the maximum load in kN, Δm is the displacement before maximum

load at ½ F_{max} in mm, and Δc is the displacement before maximum load at ¼ F_{max} in mm.

- *Dissipated energy per unit area (GD):* It is the work during cracking process divided by the fracture area. This parameter represents de adhesion force of the materials that compose the asphalt mixture.

$$GD = \frac{\int_0^{\Delta R} F(x) \cdot dx}{S} \quad (5)$$

where *GD* is the dissipated energy during cracking process in J/m^2, *F* is the load in kN, *x* is the displacement in mm, ΔR is the fracture displacement at F = 0.1 kN post-peak load in mm, and *S* is the fracture area in m^2.

- *Toughness index (TI):* it represents the toughness of asphalt mixtures, this is, the ability of keeping the components together after the maximum load has been reached or when cracking process has started.

$$TI = \frac{\int_{\Delta Fmax}^{\Delta R} F(x) \cdot dx}{S} \times (\Delta_{mdp} - \Delta_{Fmax}) I_T = \frac{W_D - W_{Fmax}}{Ab} \times (\Delta_{mdp} - \Delta_{Fmax}) \quad (6)$$

where *TI* is the toughness index in J mm/m^2, Δ_{Fmax} is the displacement at F_{max} in mm, Δ_{mdp} is the displacement after maximum load at ½ F_{max} in mm, and *S* is the fracture area in m^2. Finally, with the purpose of evaluating the influence of fibre content and test temperature on the cracking resistance of asphalt mixtures, three Fenix samples for each type of asphalt mixture (see Table 1) were tested at four different temperatures: −10, 0, 10 and 20 °C. In total, more than 60 Fenix samples were tested.

3. Results and discussion

3.1. Morphology of steel wool fibres before and after mixing and compaction

In Fig. 5(a) and (b) obtained by SEM, the surface aspect and cross section of the fibres used in the study can be seen. In this Figure, it can be observed that steel wool fibres presented some defects in their longitudinal and cross section. This was due to the fact that fibres were cut from steel wires with a bigger diameter (of approximately 2.5 mm). The blades used to cut the fibres were subjected to different types of vibrations, which produced flaws on the surface of the fibres (see Fig. 5(a)). Additionally, cross section of the fibres presented different diameters depending on the vibration of the cut (see Fig. 5(b)). In this study, the maximum diameter value of the fibres (0.157 mm) has been considered as representative value because it implies the highest contact surface with the matrix. In Fig. 5(c) and (d), damaged fibres due to crushing and cutting forces can be seen. This proves that steel wool fibres can be damaged due to mixing processes and Marshall compaction.

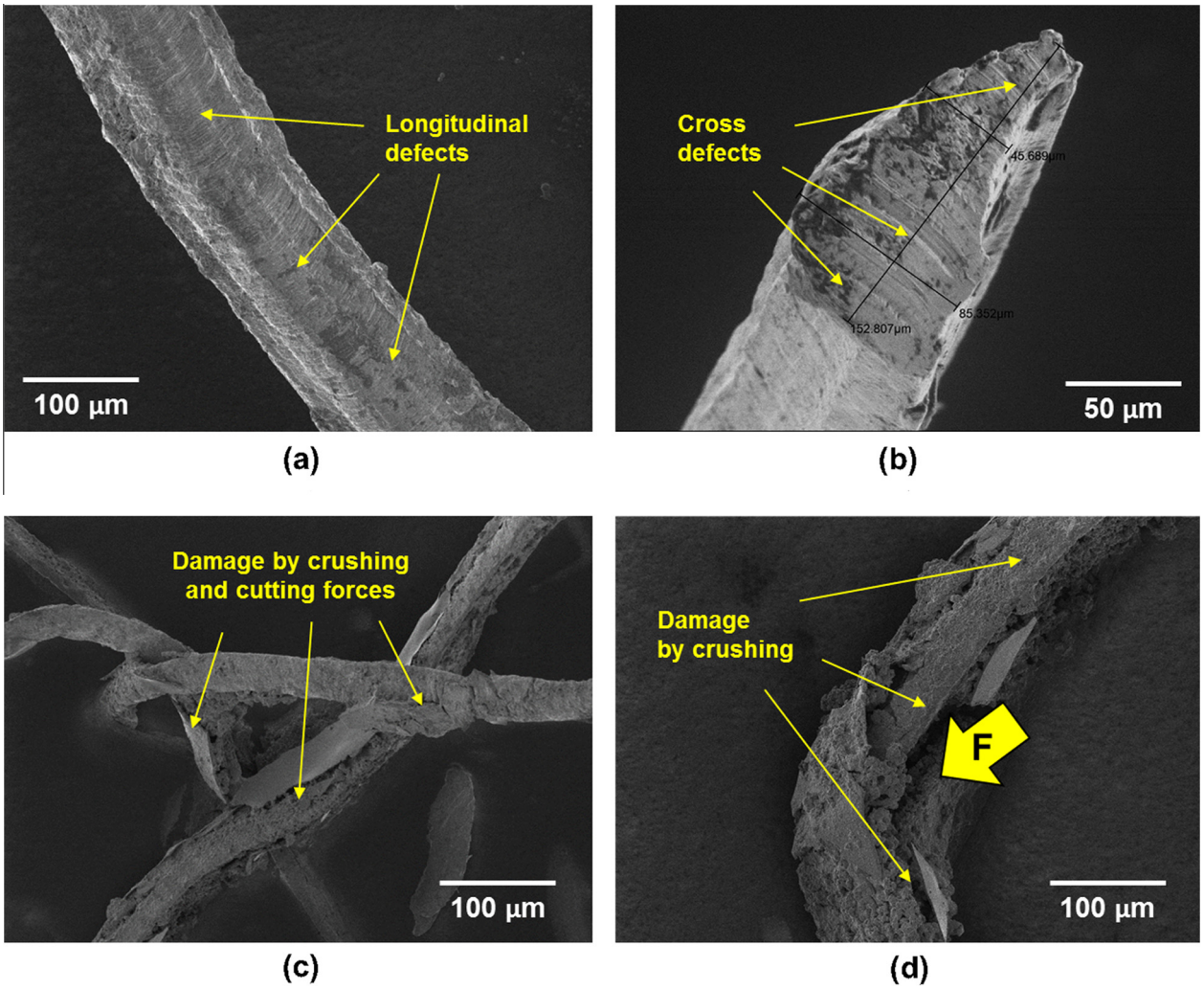

Fig. 5. SEM images of steel wool fibres (a and b) before and (c and d) after mixing and compaction process.

Considering fibres are thick and with medium length, they have bigger specific contact surface, making them more susceptible to mixing processes and compaction using the Marshall Hammer.

3.2. Distribution of fibres within asphalt mixture microstructure

Volumetric fractions of phases present in the asphalt mixtures under study as determined by the analysis of computerized tomography scan data are shown in Table 3. Although different average porosity fractions were measured for mixture designs having different fibre contents, the differences are not significant considering within mixture design variations. In addition, no clear correlation between fibre content and porosity could be stablished from these results alone. Despite the small sample size imposed by the instrument geometry, results for volumetric fraction of aggregates and bitumen show good agreement with fractions expected from mixture design, with average bitumen content remaining constant across designs. In this analysis, the variance of the fibre content, expressed as a volumetric fraction of the bitumen, was seen to increase with increasing mixture fibre content. The smaller scale analysis of the distribution of fibre contents confirm the previous result. As seen in Fig. 6, within the range of fibre contents studied, the frequency distribution of the local fibre volume fraction can be described using a folded normal distribution function (fibre content cannot be negative), the standard deviation of which increases with increasing mean fibre content. As a consequence of this higher variance, the microstructure of mixtures having larger fibre contents is expected to present zones where fibres pack together

Table 3
Volumetric fractions of phases identified in CT-Scans of asphalt mixture samples.

Design fibre content	Specimen data					Phase fractions (volumetric)									
		Sampled volume		Sub-samples volume		Porosity of total		Aggregate of total		Bitumen of total		Fibres			
												of total		of Bitumen	
%	n	voxels·10^6	cm^3	n	cm^3	%	SD%	%	SD%	%	SD%	%	SD%	%	SD%
2	2	171.6	3.30	12	1.65	6.83	1.76	81.32	3.72	11.63	2.09	0.22	0.04	1.90	0.35
4	2	171.6	3.30	12	1.65	4.92	1.79	82.62	2.35	11.67	1.27	0.50	0.09	4.29	0.74
6	2	171.6	3.30	12	1.65	7.34	1.26	81.49	2.52	10.58	1.45	0.67	0.08	6.38	0.79
8	2	171.6	3.30	12	1.65	6.50	1.60	82.34	2.80	10.14	1.51	0.81	0.17	7.95	1.65

SD: Standard Deviation, n: number of samples or sub-samples volumetric fractions.

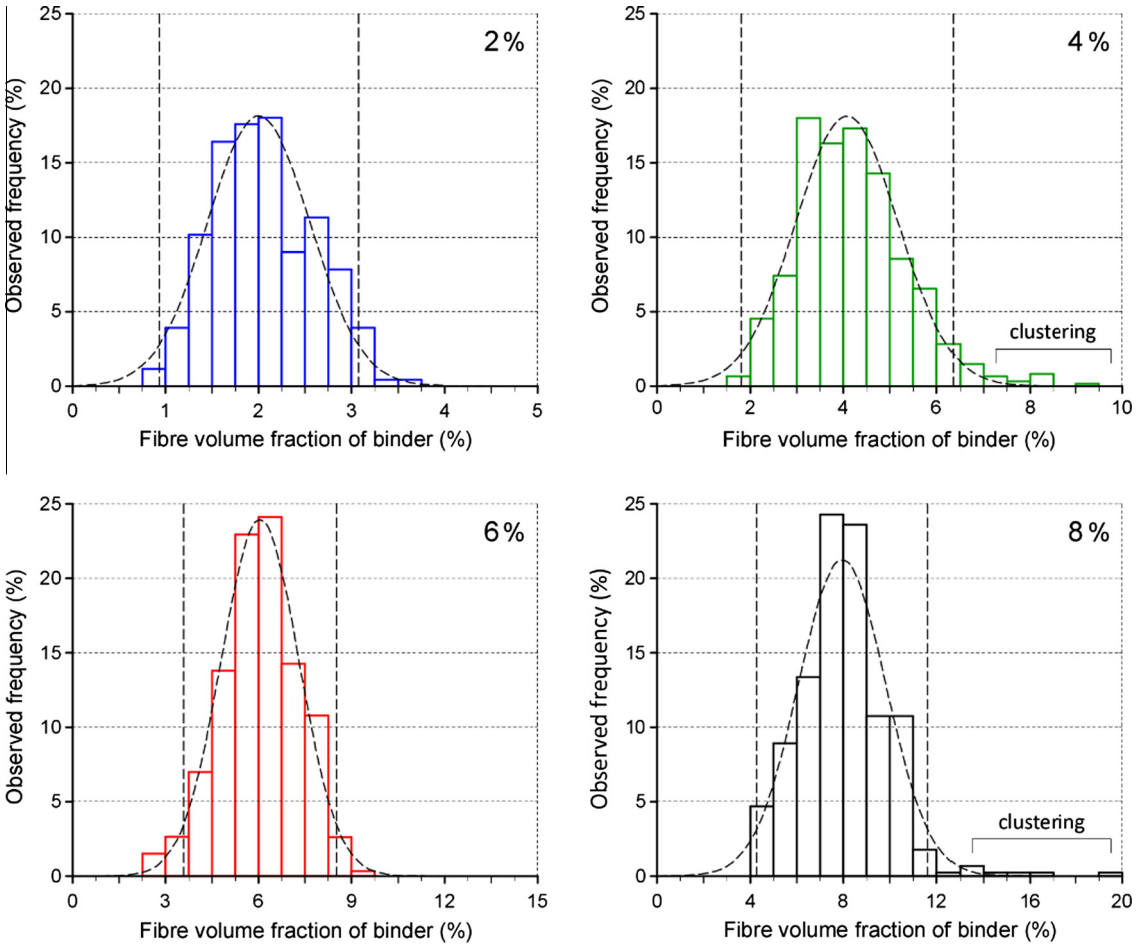

Fig. 6. Distribution of steel wool fibres within asphalt mixture microstructure as determined by analysis of Micro Computerized Tomography of mixture samples with fibre contents of 2%, 4%, 6% and 8% of bitumen volume.

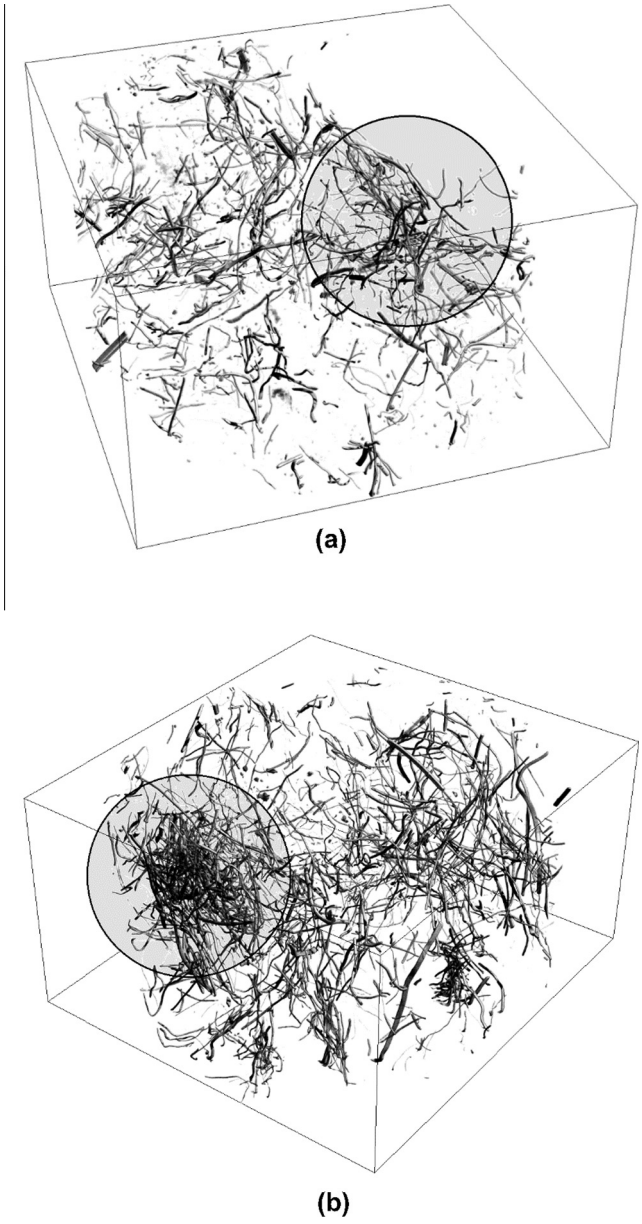

Fig. 7. 3D models of fibres within a specimen of an asphalt mixture with a fibre content of (a) 4%, and (b) 8%, by volume of bitumen, showing clustering of fibres (greyed area). Bounding box dimensions are 25 × 25 × 12 mm approximately.

forming dense fibre clusters. This clustering behaviour was observed in 2 out of 8 samples, and their presence is revealed in the distribution graphs of mixtures having 4% and 8% mean fibre content (see Fig. 6) and in the 3D models of these two samples (see Fig. 7(a) and (b)).

3.3. Effect of the fibres on the physical properties of asphalt mixtures

Bulk density and air voids content of asphalt mixtures with different percentages of fibres are shown in Fig. 8. In this Figure it can be observed that the relationship between the air voids content and the bulk density is linear and proportional to the amount of air voids in the mixture. The mixtures with higher average density were those without fibres (2.362 g/cm^3), while those with higher percentage of fibres showed lower average densities: 2.326 g/cm^3, 2.323 g/cm^3, 2.319 g/cm^3, and 2.303 g/cm^3 for mixtures with 2%, 4%, 6% and 8% of fibres, respectively. The reason for this is that

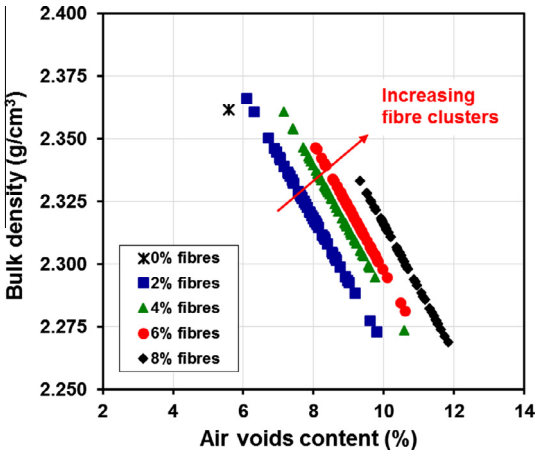

Fig. 8. Effect of fibres content on the bulk density of asphalt test samples.

the amount of bitumen and aggregates was maintained constant in the mixture, while the amount of fibres changed (see Table 1). In this way, compaction was difficult and the total air voids content increased with the amount of fibres added to the mixture. In the Marshall specimens without fibres, the average air voids content was 5.58%, while in the mixtures with 2%, 4%, 6% and 8%, the average air voids content was 7.86%, 8.63%, 9.14% and 10.49%, respectively. Moreover, mixtures with an 8% of fibre content were difficult to mix and fibre clusters were observed (see Fig. 7(b)). This happened due to that asphalt mixtures with higher fibre content are more likely to have long fibres and therefore a higher increase of the total volume due to the formation of clusters into the mixture [17].

3.4. Influence of water damage on the particle loss resistance of asphalt mixtures with fibres

Fig. 9 shows the relationship between particle loss and air voids content of the asphalt mixtures as tested after two different pre-treatments: dry conditions (Fig. 9(a)) and water damage (Fig. 9(b)). It can be observed that, for each mixture type the particle loss increases exponentially with the increase of air voids content. It can also be observed that an increase on the fibres content reduced the total particle loss in the test specimens. However, particle loss percentages of asphalt mixtures with and without fibres can change depending on the type of pre-treatment applied to the material. Comparing Fig. 9(a) and (b), it can be observed that dry conditioned specimens showed a relatively higher particle loss resistance than wet pre-treated specimens. For example, asphalt mixtures with 2% fibres and 7.86% air void content, tested under dry conditions, showed 11.6% of average particle loss, while the average particle loss of the same asphalt mixture tested under water damage was approximately 12.8%.

Likewise, asphalt mixtures with 4% and 8% fibres tested under dry conditions reached 10% of average particle loss, while results under water damage were approximately 10.8% and 11.5%, respectively. In short, water damage reduced the particle loss resistance of asphalt mixtures with fibres. This happens because the contact angle between water and bitumen is relatively small and water can penetrate in the interface between the binder and the aggregates, reducing the adhesion properties of material [3].

Furthermore, it can be concluded that steel wool fibres improve the particle loss resistance properties of asphalt mixture, although this relatively higher resistance increase is not significant. In order to evaluate the influence of the water damage compared to the dry conditions on asphalt mixtures with fibres, a Water Damage Factor

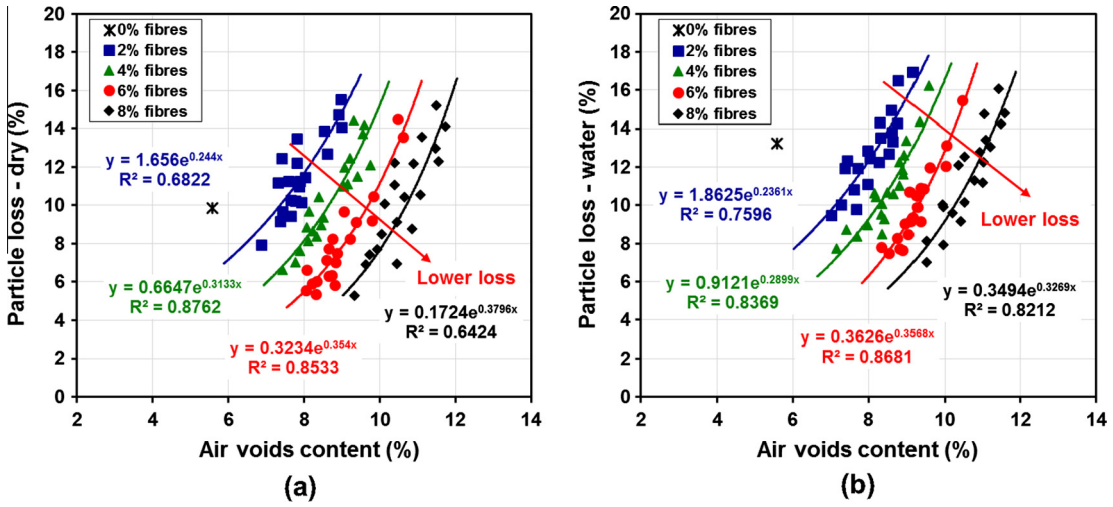

Fig. 9. Particle loss percentage of test samples with different fibre contents versus air voids content for (a) dry conditions, and (b) water conditions.

(WDF) has been defined as the relationship between the particle loss of a specimen tested under water damage conditions (*PL% water-damage*) and the particle loss value of the specimens tested under dry conditions (*PL% dry-conditions*) with the same air void content:

$$WDF = \frac{PL\%\ water\text{-}damage}{PL\%\ dry\text{-}condition} \tag{7}$$

In Fig. 10(a) the average Water Damage Factors (WDFs) obtained for the different asphalt mixtures with fibres are shown. From this Figure it can be observed that average WDF was higher to 1 in all mixtures evaluated, and that in asphalt mixtures with 6% the water damage was the highest (average WDF 1.239), followed by 8% (average WDF 1.153), 2% (average WDF 1.100) and 4% fibres (average WDF 1.052), respectively. For example, asphalt mixtures with 6% fibres recorded an increase of 19.30% of the particle loss compared to the average particle loss evaluated under dry conditions. However, observing the error bars from these data, it is still unclear if steel wool fibres in asphalt mixture can significantly reduce the effect of water damage on particle loss. With this purpose, in Fig. 10(b), the Weibull probability of all the calculated WDFs has been calculated and presented against the data percentiles. The Weibull probability distribution function was used in this study considering that the particle loss phenomenon in asphalt mixtures occurred due to the microcracking that happen during each loading cycle [22]. So, when impacts are repeated during the tests and due to the accumulated damage, cracks that separate the aggregates from the matrix can appear (see damaged specimen in Fig. 3). Thus, the particle loss data can be modelled as a mechanical fracture process of aggregate of the mixture, adjusted to a probability distribution of Weibull type [26]. From Fig. 10(b), it can be observed that the relationship between the Weibull probability and the data percentiles is linear for the water damage factors data. This means that the WDFs can be represented by a single Weibull distribution function, and that the variability of this function happens due to the scatter, not to the amount of fibres in the mixture. For this reason, it can be confirmed that steel wool fibres do not contribute to improve the water damage resistance of asphalt mixture.

3.5. Influence of fibre content on the stiffness modulus of asphalt mixtures

The effect of fibre content on stiffness modulus depending on the asphalt mixture temperatures and air voids content can be observed in Fig. 11(a) and (b), respectively. In Fig. 11(a) it can be observed that the stiffness modulus registered by the asphalt mixtures decreased with increasing of the test temperature, from 0 °C

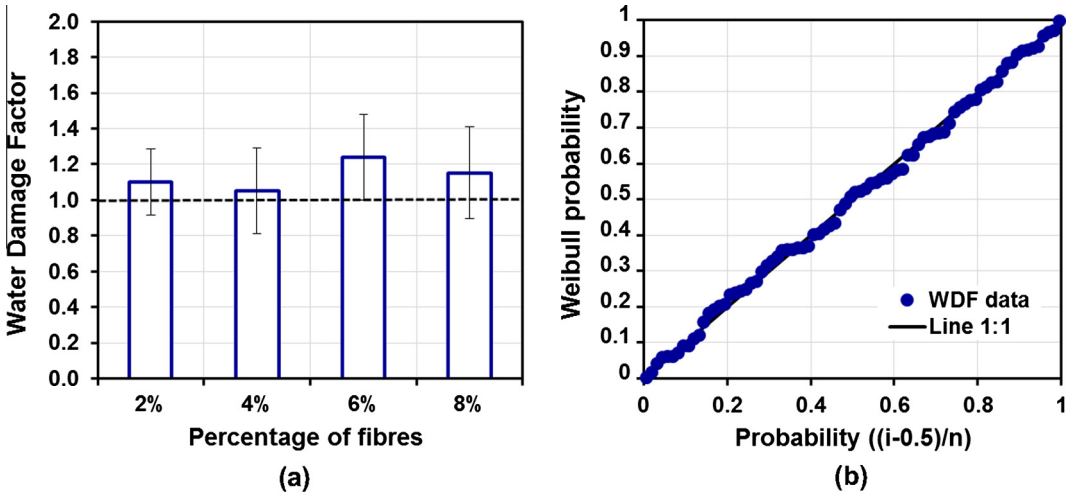

Fig. 10. (a) Average Water Damage Factors versus percentage of fibres. (b) Probability-probability plot of WDFs data. The error bars represent the standard deviation of the measurements.

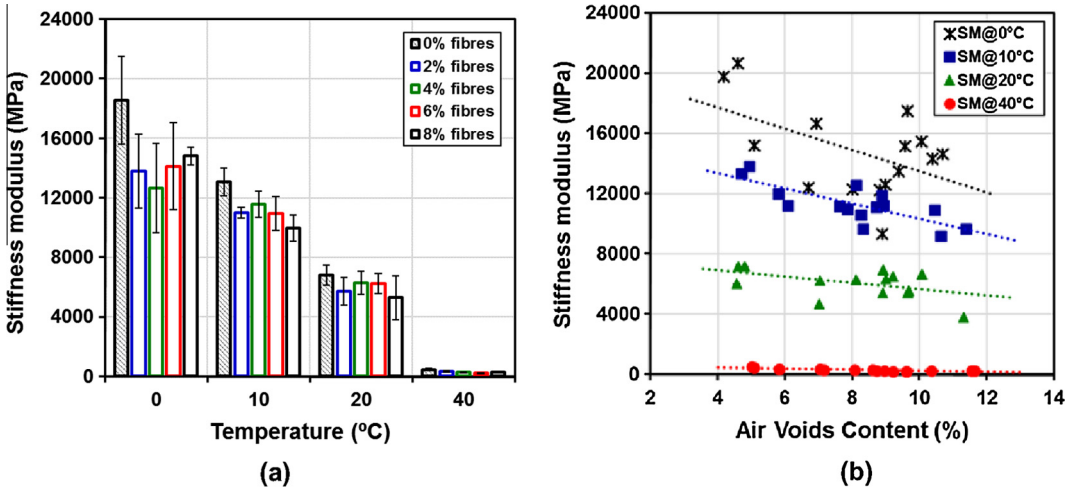

Fig. 11. Stiffness modulus results of test specimens versus (a) test temperature and (b) air voids content. The error bars represent the standard deviation of the measurements.

to 40 °C. At low temperatures (0 °C), it can be observed that the presence of steel wool fibres decrease the stiffness modulus of asphalt mixtures respect to the asphalt mixtures without fibres. However, when the test temperature increases, this difference in stiffness modulus between the asphalt mixtures with and without fibres is reduced (see Fig. 11(a)). For example, asphalt mixtures with 0% and 4% fibres, tested at a temperature of 0 °C, shows an average stiffness modulus of 18,540 MPa and 12,664 MPa, respectively; while the average stiffness modulus of the same asphalt mixtures tested at a temperature of 20 °C was of 6788 MPa and 6278 MPa, respectively. This is explained due to the visco-elastic behaviour of bitumen, which undergoes a loss of stiffness when the temperature increases (from 0 °C to 20 °C), thus resulting in a decrease in the viscosity of asphalt mixture composites and consequent reduction of the stiffness modulus. Moreover, from Fig. 11 (b), it can be observed that independently of the fibre content, the stiffness modulus slightly reduces with the increase of the air voids content, although it increases with the reduction of the temperature because of hardening of the bitumen (from 40 °C to 0 °C). Moreover, Fig. 12(a) shows the relationship between all the stiffness modulus values measured by indirect tensile on the test specimens in the longitudinal (A-A′) and cross (B-B′) directions, respectively. From this Figure it can be observed that independently of the fibre content and test temperature, the stiffness modulus measured in both directions (A and B) were very similar for most of the asphalt specimens tested. This proves that asphalt mixtures reinforced with fibres do not present an anisotropic mechanical behaviour for the plane orthogonal to the coaxial axis, which can directly affect the average stiffness modulus. Additionally, this result also proves that at the dimensional scale of the test specimens the fibre distribution inside the asphalt mixtures can be considered uniform, not presenting a negative influence on the stiffness modulus value. In summary, it can be concluded that steel wool fibres do not improve the stiffness modulus of asphalt mixtures respect to the asphalt mixtures without fibres. In order to prove that the fibre content does not have a significant influence on the stiffness modulus of asphalt mixture, regardless of test temperature, a ratio between the stiffness modulus of all the test specimens with steel wool fibres and the stiffness modulus of the mixture without fibres, tested at the same temperature, has been calculated (see Fig. 12). For simplicity reason, these data have not been presented in the paper. However, to prove that the difference between them is due to the scatter (see error bars in Fig. 11 (a)), the normal probability of these values has been calculated

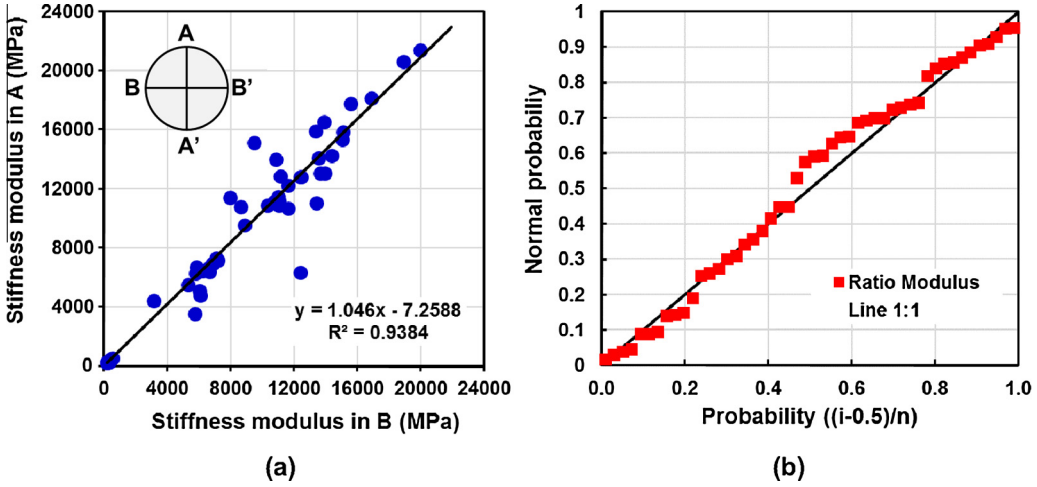

Fig. 12. (a) Relationship between stiffness modulus of the test specimens measured in longitudinal (A) and cross (B) directions. (b) Probability-probability plot of the ratio between the stiffness modulus of the test specimens with fibres and the stiffness modulus of the asphalt mixture without fibres, at different temperatures.

and presented against the data percentiles in Fig. 12(b). Results shown that data can be aligned in a straight line with a 1:1 slope. This means that the differences in the stiffness modulus between tests specimens with and without steel wool fibres are due to statistical variations, and that the fibre content or the test temperature does not have a significant influence on the stiffness modulus of the asphalt mixtures.

3.6. Influence of fibre content on the cracking resistance of asphalt mixtures

Influence of fibre content on cracking resistance of asphalt mixtures can be evaluated through the parameters obtained from Fenix Test. The results obtained for each mechanical parameter have been analysed, according to test temperature used, from −10 °C to 20 °C. The effect of fibre content on Tensile Stiffness Index (TSI) and Maximum Tensile Force (F_{max}) for each test temperature are shown in Fig. 13(a) and (b), respectively. As shown in Fig. 13, the effect of fibres on TSI and F_{max} of mixtures depends on test temperature. Highest average values for TSI and F_{max} were obtained at lower temperatures, gradually decreasing with increasing test temperature. Similarly as observed in the case of stiffness modulus (see Fig. 11(a)), these results can be explained by the loss of stiffness affecting bitumen when the temperature increases, which results in a loss of viscosity of asphalt mixture composites and a consequent reduction of the material strength. At −10 °C, TSI of mixtures was observed to decrease with increasing fibre content. However, from 0 °C upwards, higher average TSI was observed for asphalt mixtures with fibres compared to reference mixture without fibres, although TSI values do not show a clear correlation with fibre content. Likewise, F_{max} of mixtures was observed to decrease with increasing fibre content at −10 °C and 0 °C (see Fig. 13(b)). However, this is not observed in the results of the tests performed at 10 °C and 20 °C where the average F_{max} of asphalt mixtures with fibres equals or exceeds the F_{max} of the reference mixture. Consequently, the influence of the fibres on the strength of mixtures depends on temperature, and reverts from negative to positive as temperature increases for both TSI and F_{max}. This is due to the fact that at lower temperatures (−10 °C and 0 °C) the asphalt mixture behaves as a rigid solid with brittle behaviour (higher TSI and F_{max} values). Under this condition, when the asphaltic mastic fails in tension, cracking propagates through the short sections of fibres exposed inside the cracks. Despite having higher intrinsic tensile strength, due to their small cross-section, at the fibre content range explored in this study fibres, do not contribute to tensile strength of asphalt mixtures at low temperatures (see tensile results of fibres in Table 4). This because fibres break together with the asphaltic mastic thus dissipating low energy during cracking process compared with a mixture without fibres. In contrast, at higher temperatures (10 °C and 20 °C), asphalt mixture presents a ductile behaviour (lower TSI and F_{max} values). Under this condition, gradual deformation of the asphalt mastic allows stress transfer to the fibres, thus behaving like a composite material. The higher intrinsic tensile strength of the fibres then contributes to higher cracking resistance and consequently in a greater or lesser dissipated energy (depending on temperature) during cracking process.

Table 4
Average results of the tensile properties of fibres with diameter 0.15 mm.

Parameter	Avg. result
Ultimate tensile strength, σ_u in (MPa)	526.59
Deformation in ultimate tensile strength, ε_u in (mm)	0.948
Elastic modulus, E in (MPa)	63776.94

To increase the understanding of this behaviour, results of Dissipated Energy (GD) and Toughness Index (TI) versus test temperature are shown in Fig. 14(a) and (b), respectively. In general, at lower test temperatures (−10 °C and 0 °C) asphalt mixtures with and without fibres required a higher energies to achieve cracking than asphalt mixtures at higher test temperatures (10 °C and 20 °C). However, asphalt mixtures at low test temperatures showed low capacity to keep the asphalt mixture components together after the maximum load has been reached and cracking process has started (lower TI values in Fig. 14(b)). In these mixtures the breakage occurs suddenly. Conversely, at higher temperatures (above 10 °C) the asphalt mixtures displayed a higher capacity to keep the components together, with the breakage occurring slowly. Asphalt mixtures at higher temperatures present a ductile behaviour and consequently a higher toughness due to their higher deformation ability (see TI values in Fig. 14(b)). In previous research using the same asphalt bitumen and mixture proportions of the reference mixture (but without fibres), it was found that toughness of asphalt mixtures increased at temperatures between 10 °C and 20 °C but decreased at temperatures below 0 °C [29]. This was explained as the effect of internal damage due to differential thermal contraction, which is consequence of the large difference in the coefficients of thermal contraction between aggregates and the asphalt mastic [30].

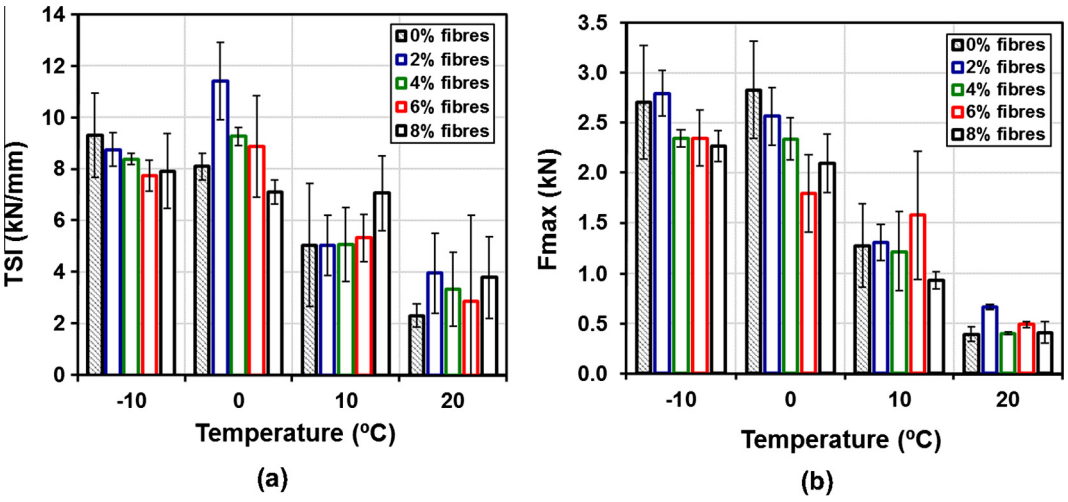

Fig. 13. Average results of (a) tensile stiffness index (TSI) and (b) maximum tensile force (Fmax) versus test temperature. The error bars represent the standard deviation of the measurements.

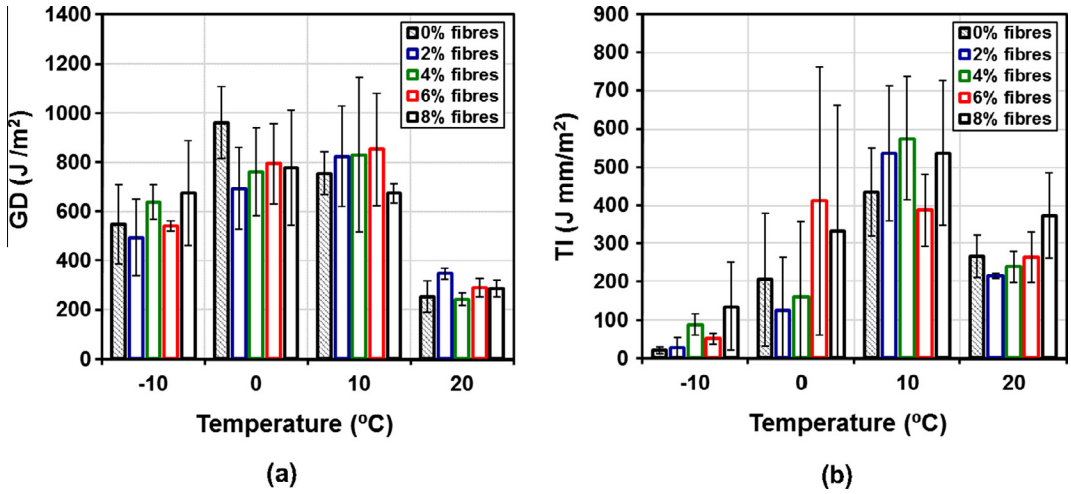

Fig. 14. Average results of (a) dissipated energy per unit area (GD) and (b) toughness index (TI) versus test temperature. The error bars represent the standard deviation of the measurements.

Furthermore, if the standard deviation of the results (represented by error bars) of TSI, F_{max}, GD and TI are analysed independently of the test temperature, it can be observed that the variability of the results between the asphalt mixtures with and without fibres was similar. That is, if one of the studied test specimens for one mechanical parameter (e.g. F_{max} in Fig. 13(b)) and one specific temperature (e.g. 10 °C) is randomly selected, the difference between an asphalt mixture without and with a certain fibre content is not significant. Consequently, it can be concluded that, within the range of fibre contents and test temperatures explored in this study, fibre content does not have a significant effect on the cracking resistance of the asphalt mixture evaluated. In order to prove this, a Maximum Force Ratio (MFR) has been defined as the relationship between maximum tensile force of a test specimen without fibres (*Fmax-without fibres*) and the maximum tensile force of the mixture reinforced with fibres (*Fmax-with fibres*), tested at the same temperature as the mixture without fibres:

$$MFR = \frac{Fmax\text{-}without\ fibres}{Fmax\text{-}with\ fibres} \quad (8)$$

In Fig. 15 the average Maximum Force Ratios (MFRs) obtained for the different asphalt mixtures with fibres versus test temperatures are shown. In this Figure it can be observed that average MRF was higher than 1 in the mixtures evaluated at temperatures of −10 °C and 0 °C, while mixtures evaluated at temperatures of 10 °C and 20 °C presented a MFR lower than 1. This means that fibre content presented higher influence on the mechanical resistance of mixtures at temperatures above 10 °C compared to asphalt mixtures without fibres. However, observing the error bars from all data, it is still unclear if steel wool fibres in asphalt mixture can significantly increase mechanical resistance of the mixtures. To prove that the difference between them is due to the scatter, the normal probability of these values has been calculated and presented against the data percentiles in Fig. 16. As it occurred with the stiffness modulus data, results showed that MFRs data can be aligned in a straight line with a 1:1 slope. This means that the differences in the maximum tensile force between tests specimens with and without steel wool fibres are due to statistical variations, and that the fibre content or the test temperature do not have a significant influence on the mechanical resistance of the asphalt mixtures. These results can be attributed to the fact that the failure mode of the fibres in the Fenix tests at test temperatures above 10 °C was mostly by pull-out of the fibres, due to the lower adherence between the fibres and asphalt matrix, as a result of the mostly smooth surface morphology of the fibres (see Fig. 5(a)). Nevertheless, in the frame of development of new fibre-reinforced asphalt mixtures with self-healing properties via microwave heating, electrically conductive steel wool fibres added into the asphalt mixture continue to be beneficial in order to increase the heating rates of the composite material.

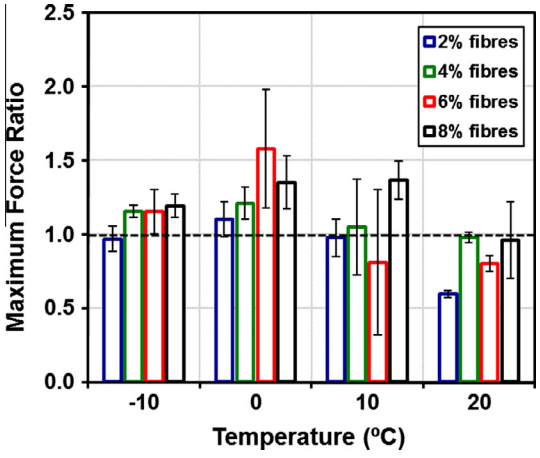

Fig. 15. Average Maximum Force Ratios (MFRs) versus test temperature. The error bars represent the standard deviation of the measurements.

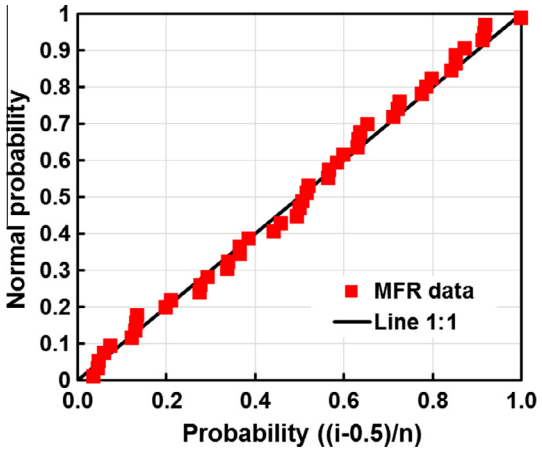

Fig. 16. Probability-probability plot of MFRs data.

4. Conclusions

This paper has quantified the effect of steel wool fibres addition on the physical and mechanical properties of asphalt mixtures with crack-healing purposes via microwave radiation. The main conclusions obtained from this work are summarized as follows:

- It was proved that steel wool fibres can be mechanically damaged due to manufacture processes. This was due to the fact that fibres are thick and with medium length so they are susceptible to the impact of aggregates during the mixing process and Marshall mechanical compaction.
- Fibre clusters existence inside of asphalt mixtures was confirmed in this study by direct detection using CT-scans of mixture samples. It was verified that the fibre distribution variation within the mixture microstructure increases as the average fibre content of the mixture increases, which resulted in the formation of dense fibre clusters. However, it seems to have no significant effect on the physical and mechanical properties of fibre-reinforced asphalt mixtures in the range of fibre contents explored in this study.
- The bulk density of asphalt mixtures with steel wool fibres proportionally reduced with the increase of the air voids content. This reduction was mainly attributed to the total volume variation of each specimen, rather than the mass variations. This, considering that the amount of bitumen and aggregates was maintained constant in the mixture, but the amount of fibres changed.
- The particle loss percentage measured on the fibre-reinforced asphalt mixtures increased exponentially with the increase of the air voids content. In general, steel wool fibres improved the particle loss resistance of mixtures. However, since air voids content increased with the fibre content, mechanical resistance increases can be significantly reduced. Based on the probability analysis it was confirmed that steel wool fibres did not contribute to improve the water damage resistance of asphalt mixture.
- Stiffness modulus measured on the fibre-reinforced asphalt mixtures reduced with the increase of the test temperature. This is because bitumen reduces its stiffness with the increase of the temperature due to its visco-elastic behaviour, which results in a loss of viscosity of asphalt mixture composites. Besides, it can be found that regardless of the fibre content, the stiffness modulus slightly reduced with the increase of the air voids content, although it increased with the reduction of the temperature because of hardening of the bitumen. In short, based on the probability analysis it was proven that the fibre content or the test temperature do not have a significant influence on the stiffness modulus of the asphalt mixtures.
- Based on a probability analysis it was confirmed that steel wool fibres did not significantly contribute to improve the cracking resistance properties of the asphalt mixtures evaluated under different test temperatures. Nevertheless, based on the previous work by Norambuena-Contreras and Garcia [23], steel wool fibres added into the asphalt mixture continue to be beneficial in order to increase the heating rates of the asphalt mixtures with crack-healing purposes via microwave radiation.

Acknowledgements

Authors acknowledge the financial support given by the National Commission for Scientific & Technological Research (CONICYT) from the Government of Chile, through the Research Project FONDECYT Initiation 2014 N°11140103 and FONDEQUIP project EQM130028, which enabled to perform Micro-CT observations. Additionally, the authors would also like to acknowledge the experimental help provided by the bachelor students Jose Careaga, Maria Jose San Martin and Camila Sanhueza, from the Department of Civil and Environmental Engineering at the University of Bío-Bío. Finally, the authors wish to express their gratitude to Irene Gonzalez-Torre from the LabMat-UBB for her contribution to improve this paper.

References

[1] G. Thenoux, A. González, R. Dowling, Energy consumption comparison for different asphalt pavements rehabilitation techniques used in Chile, Resour. Conserv. Recy. 49 (2007) 325–339.
[2] G.D. Airey, State of the art report on ageing test methods for bituminous pavement materials, Int. J. Pavement Eng. 4 (3) (2003) 165–176.
[3] G.D. Airey, Y.-K. Choi, State of the art report on moisture sensitivity test methods for bituminous pavement materials, Int. J. Road Mater. Pavement Des. 3 (4) (2002) 355–372.
[4] J. Norambuena-Contreras, I. Gonzalez-Torre, Influence of geosynthetic type on retarding cracking in asphalt pavements, Constr. Build. Mater. 78 (2015) 421–429.
[5] S.M. Abtahi, M. Sheikhzadeh, S.M. Hejazi, Fibre-reinforced asphalt-concrete – A review, Constr. Build. Mater. 24 (6) (2010) 871–877.
[6] R.S. McDaniel, NCHRP Synthesis 475: Fibre Additives in Asphalt Mixtures, Report to American Association of State Highway and Transportation Officials, Transportation Research Board, Washington DC, USA, 2015.
[7] H. Hassan, S. Al-Oraimi, R. Taha, Evaluation of open-graded fiction come mixtures containing cellulose fibres and styrene butadiene rubber polymer, J. Mater. Civ. Eng. 17 (4) (2005) 415–422.
[8] S. Wu, Q. Ye, N. Li, Investigation of rheological and fatigue properties of asphalt mixtures containing polyester fibres, Constr. Build. Mater. 22 (10) (2008) 2111–2115.
[9] B.J. Putman, S.N. Amirkhanian, Utilization of waste fibres in stone matrix asphalt mixtures, resources, Conserv. Recy. 42 (2004) 265–274.
[10] R.L. Fitzgerald, Novel Applications of Carbon Fibre for Hot Mix Asphalt Reinforcement and Carbon-Carbon pre-forms (M.Sc. thesis), Michigan Technological University, USA, 2000.
[11] A. Maurer Dean, M. Gerald, Field performance of fabrics and fibres to retard reflective cracking, Transp. Res. Rec. 1248 (1989) 13–23.
[12] A. García, E. Schlangen, M. van de Ven, Q. Liu, Electrical conductivity of asphalt mortar containing conductive fibers and fillers, Constr. Build. Mater. 23 (10) (2009) 3175–3181.
[13] A. García, J. Norambuena-Contreras, M.N. Partl, Experimental evaluation of dense asphalt concrete properties for induction heating purposes, Constr. Build. Mater. 46 (2013) 48–54.
[14] A. Garcia, E. Schlangen, M. Van de Ven, Two ways of closing cracks on asphalt concrete pavements: microcapsules and induction heating, Key Eng. Mater. 417 (2009) 573–576.
[15] E. Schlangen, A. García, M. van de Ven, G. van Bochove, J. van Monfort, Q. Liu, Highway A58: The first engineered self-healing asphalt road, in: 3rd International Conference on Self-Healing Materials, Bath, United Kingdom. 2011.
[16] A. Garcia, Self-healing of open cracks in asphalt mastic, Fuel 93 (2012) 264–272.
[17] A. Garcia, J. Norambuena-Contreras, M.N. Partl, P. Schuetz, Uniformity and mechanical properties of dense asphalt concrete with steel wool fibres, Constr. Build. Mater. 43 (2013) 107–117.
[18] A. Garcia, M. Bueno, J. Norambuena-Contreras, M.N. Partl, Induction heating of dense asphalt concrete, Constr. Build. Mater. 49 (2013) 1–7.
[19] A. Garcia, M. Bueno, J. Norambuena-Contreras, M.N. Partl, Single and multiple healing of porous and dense asphalt concrete, J. Intel. Mat. Syst. Struct. 26 (2015) 425–433.
[20] J. Gallego, Miguel A. del Val, V. Contreras, A. Paez, Heating asphalt concrete with microwaves to promote self-healing, Constr. Build. Mater. 42 (2013) 1–4.
[21] J. Norambuena-Contreras, J.L. Concha, Self-Healing of Asphalt Mixtures Via Microwave Heating: 2016 ISAP Symposium, ISAP2016, Jackson Hole, Wyoming, USA, 2016.
[22] J. Norambuena-Contreras, V. Gutierrez, I. Gonzalez-Torre, Physical and mechanical behaviour of a fibre-reinforced membrane with self-healing purposes via microwave heating, Constr. Build. Mater. 94 (2015) 45–56.
[23] J. Norambuena-Contreras, A. Garcia, Self-healing of asphalt mixture by microwave and induction heating, Mater. Design 106 (2016) 404–414.
[24] MOP. Manual de carreteras, vol. 5, Revestimientos y Pavimentos: Mezclas asfálticas en caliente. Santiago, Ministerio de Obras Públicas, Chile. 2014.
[25] EN 12697-17: 2004+A1:2007. Bituminous mixtures – Test methods for hot mix asphalt – Part 17: Particle loss of porous asphalt specimen. European Committee for Standardization (CEN), Brussels, Belgium.
[26] A. García, J. Norambuena-Contreras, M.N. Partl, A parametric study on the influence of steel wool fibres in dense asphalt concrete, Mater. Struct. 47 (9) (2014) 1559–1571.

[27] EN 12697-26:2012 (Annex C). Bituminous mixtures. Test methods for hot mix asphalt. Part 26: Stiffness. European Committee for Standardization (CEN), Brussels, Belgium.
[28] J. Norambuena-Contreras, D. Castro-Fresno, A. Vega-Zamanillo, M. Celaya, I. Lombillo-Vozmediano, Dynamic modulus of asphalt mixture by ultrasonic direct test, NDT&E Int. 43 (7) (2010) 629–634.
[29] G. Valdes, A. Calabi Floody, R. Miró Recasens, J. Norambuena-Contreras, Mechanical behaviour of asphalt mixtures with different aggregate type, Constr. Build. Mater. 101 (2015) 474–481.
[30] K.W. Kim, M. El Hussein, Variation of fracture toughness of asphalt concrete under low temperatures, Constr. Build. Mater. 11 (7–8) (1997) 403–411.